

Simulated bifurcation for higher-order cost functions

Taro Kanao^{a)} and Hayato Goto

Frontier Research Laboratory, Corporate Research & Development Center, Toshiba Corporation, 1, Komukai-Toshiba-cho, Saiwai-ku, Kawasaki 212-8582, Japan

(Dated: 30 November 2022)

High-performance Ising machines for solving combinatorial optimization problems have been developed with digital processors implementing heuristic algorithms such as simulated bifurcation (SB). Although Ising machines have been designed for second-order cost functions, there are practical problems expressed naturally by higher-order cost functions. In this work, we extend SB to such higher-order cost functions. By solving a problem having third-order cost functions, we show that the higher-order SB can outperform not only the second-order SB with additional spin variables, but also simulated annealing applied directly to the third-order cost functions. This result suggests that the higher-order SB can be practically useful.

Special purpose hardware solvers for the Ising problem¹ have been applied to combinatorial optimization problems². Such hardware solvers are referred to as Ising machines³. Ising machines with analogue computers have attracted attention, such as quantum annealers⁴ with superconducting circuits⁵ and coherent Ising machines with pulse lasers⁶. Also, Ising machines with digital processors have been developed based on, e.g., simulated annealing (SA)^{7–9}, simulated bifurcation (SB)¹⁰, and other algorithms¹¹.

SB is a heuristic algorithm based on numerical simulation of a classical counterpart of a quantum bifurcation machine, which is a quantum annealer using nonlinear oscillators^{12–15}. SB allows us to simultaneously update variables, and thus can easily be accelerated by parallel processing with, e.g., graphics processing units (GPUs) and field-programmable gate arrays (FPGAs)^{10,16–18}. Two improved variants of SB have been reported: ballistic and discrete SBs (bSB and dSB)¹⁹. In addition, bSB and dSB with thermal fluctuations have been studied²⁰. SB has been benchmarked against other Ising machines^{21,22}. Besides, SB has been applied to financial portfolio optimizations^{23,24}, financial trading machines²⁵, traveling salesman problems²⁶, clustering with a hybrid method²⁷, and wireless communications²⁸.

In the Ising problem, the aim is to minimize cost functions written in second-order polynomials of spin variables, for which Ising machines have been designed. However, some combinatorial optimization problems are naturally expressed by cost functions with higher-order polynomials than second order (higher-order cost functions). To apply Ising machines to such problems, higher-order cost functions have been transformed to second-order ones^{29–33}, though such transformations usually require additional spin variables and thus increase computational costs.

In this work, we extend SB to apply it directly to a problem with higher-order cost functions. Since SB is based on simulation, this approach can easily be implemented. To benchmark the higher-order SB, we use

a three-regular three-XORSAT (3R3X) problem^{22,34–36}, because this problem yields third-order cost functions and its solution can be known in advance. We compare the third-order SB with that transformed to second order. As a result, we find that third-order bSB and dSB (3bSB and 3dSB) show higher performance than the second-order ones (2bSB and 2dSB). Surprisingly, 3bSB performs better than 3dSB, while 2dSB does better than 2bSB as in the previous study¹⁹. We further find that 3bSB can be superior to SA applied directly to the third-order cost functions. These results suggest that the higher-order SB will offer another useful approach to special purpose hardware solvers for combinatorial optimization problems.

A third-order cost function with N spin variables $s_i = \pm 1$ can generally be written as

$$E(\mathbf{s}) = -\sum_i h_i s_i - \sum_{i,j} J_{ij} s_i s_j - \sum_{i,j,k} K_{ijk} s_i s_j s_k, \quad (1)$$

where \mathbf{s} is a vector consisting of s_i , and h_i , J_{ij} , and K_{ijk} are coefficients. Since $s_i^2 = 1$, we assume without loss of generality that $J_{ii} = 0$, and $K_{ijk} = 0$ if two of i , j , and k are equal.

We here extend second-order bSB and dSB to third-order ones. The third-order bSB and dSB are based on the following equations of motion for positions x_i and momenta y_i corresponding to s_i :

$$\dot{y}_i = -[a_0 - a(t)]x_i + c f_i, \quad (2)$$

$$\dot{x}_i = a_0 y_i, \quad (3)$$

where the dots denote time derivatives, a_0 is a constant parameter, $a(t)$ is a bifurcation parameter increased from 0 to a_0 with the time t , and c is a normalization factor determined from forces f_i . The forces f_i are given by

$$f_i = -\frac{\partial E(\mathbf{x})}{\partial x_i} = G_i(\mathbf{x}) \quad (\text{bSB}), \quad (4)$$

$$f_i = -\frac{\partial E(\mathbf{x})}{\partial x_i} \Big|_{\mathbf{x}=\mathbf{s}} = G_i(\mathbf{s}) \quad (\text{dSB}). \quad (5)$$

For 3bSB, f_i are the gradients $G_i(\mathbf{x})$ of $E(\mathbf{x})$, while for 3dSB, \mathbf{x} in the gradients is substituted by \mathbf{s} , which is a vector of the signs of x_i , $s_i = \text{sgn}(x_i)$. Both 3bSB

^{a)} taro.kanao@toshiba.co.jp

and 3dSB assume perfectly inelastic walls at $x_i = \pm 1$ ¹⁹, that is, if $|x_i| > 1$, x_i and y_i are set to $\text{sgn}(x_i)$ and 0, respectively. Equations (2) and (3) are solved with the symplectic Euler method³⁷, which discretizes the time with an interval Δt and computes time evolutions of x_i and y_i step by step. The signs of x_i at the final time give a solution. The solution at least corresponds to a local minimum of $E(\mathbf{s})$ as for 2bSB and 2dSB¹⁹, because Eq. (2) becomes $\dot{y}_i = c_0 f_i$ at the final time. Note that when all K_{ijk} are zero in Eq. (1), Eqs. (2)-(5) reproduce 2bSB and 2dSB in Ref. 19. We thus focus on the third term in Eq. (1) in the following.

To reduce the computational cost of calculating f_i , we utilize sparse connectivity of the 3R3X problem, that is, the number, M , of nonzero K_{ijk} is much smaller than the total number of K_{ijk} . We expect that sparse connectivities often appear in applications and therefore the following method will be useful. By denoting nonzero K_{ijk} by K_m ($m = 1, 2, \dots, M$), $E(\mathbf{s})$ is expressed as

$$E(\mathbf{s}) = - \sum_{m=1}^M K_m s_{v_{m1}} s_{v_{m2}} s_{v_{m3}}, \quad (6)$$

where v_{mn} with $n = 1, 2, 3$ represent the indices of spin variables included in the m th term. To further reduce the time required for evaluating the third-order SB, we calculate the gradients by

$$G_i(\mathbf{x}) = \frac{1}{x_i + \epsilon} \sum_{m=1}^M a_{im} K_m x_{v_{m1}} x_{v_{m2}} x_{v_{m3}} \quad (\text{bSB}), \quad (7)$$

$$G_i(\mathbf{s}) = s_i \sum_{m=1}^M a_{im} K_m s_{v_{m1}} s_{v_{m2}} s_{v_{m3}} \quad (\text{dSB}), \quad (8)$$

$$a_{im} = \delta_{i,v_{m1}} + \delta_{i,v_{m2}} + \delta_{i,v_{m3}}, \quad (9)$$

where $\delta_{i,j}$ is 1 if $i = j$ and otherwise 0. Equation (8) exactly gives the derivative in Eq. (5), because a_{im} pick up terms including s_i from Eq. (6), and these s_i are canceled by multiplying s_i in Eq. (8) with $s_i^2 = 1$. This method is valid since Eq. (6) is linear with respect to each s_i . Similarly, Eq. (7) yields the same value as Eq. (4) if $x_i \neq 0$ and $\epsilon = 0$. To stabilize calculations, we set $\epsilon = 10^{-14}$. We empirically found that Eqs. (7) and (8) could reduce the evaluation time compared with direct differentiation, which may be because these equations gather three terms derived from $x_{v_{m1}} x_{v_{m2}} x_{v_{m3}}$ together and thus reduce memory accesses for $x_{v_{mn}}$ and $s_{v_{mn}}$.

The 3R3X problem is mapped to a minimization problem of Eq. (6) with the following v_{mn} and K_m ³⁴. Here, M equals N . For each of $n = 1, 2, 3$, the vector of indices v_{mn} is a permutation of $1, 2, \dots, N$. For each m , three indices v_{m1} , v_{m2} , and v_{m3} are different from each other. For different m , the combinations of v_{m1} , v_{m2} , and v_{m3} are different. K_m is given by $(-1)^{b_m}$ with $b_m = 0, 1$. Thus $E(\mathbf{s}) \geq -N$ holds.

For a 3R3X instance, a solution \mathbf{s}_0 minimizing $E(\mathbf{s})$ can be obtained with linear algebra³⁴, that is, \mathbf{s}_0 is re-

lated to a solution, $\xi_i = 0, 1$, of linear equations,

$$\sum_{i=1}^N a_{mi} \xi_i = b_m, \quad \text{mod } 2, \quad (10)$$

by $s_{i0} = (-1)^{\xi_i}$. However, depending on a_{mi} and b_m , Eq. (10) may have no solution. To ensure that Eq. (10) has at least one solution, we instead give a_{mi} and ξ_i , and determine b_m with Eq. (10). Then an exact solution \mathbf{s}_0 is indicated by $E(\mathbf{s}_0) = -N$.

A third-order cost function of the 3R3X problem can be decomposed to second-order one by mapping a term $-(-1)^b s_1 s_2 s_3$ to

$$h(s_1 + s_2 + s_3) + \tilde{h}\tilde{s} + J(s_1 s_2 + s_2 s_3 + s_3 s_1) + \tilde{J}(s_1 + s_2 + s_3)\tilde{s}, \quad (11)$$

where $\tilde{s} = \pm 1$ is an ancillary spin variable, and J , \tilde{J} , h , and \tilde{h} are coefficients determined so that s_1 , s_2 , and s_3 minimizing Eq. (11) coincide with ones minimizing $-(-1)^b s_1 s_2 s_3$ ^{29,34,38}. We use $J = 1/4$, $\tilde{J} = (-1)^b/2$, $h = -(-1)^b/4$, and $\tilde{h} = -1/2$, which normalize the minimum of Eq. (11) to -1 . The ancillary spin variables increase the total number of spin variables to $2N$.

We also directly apply SA to third-order cost functions (3SA). In an update in SA⁷, one calculates a change in a cost function ΔE_i caused by a flip of s_i . The flip is accepted if $\beta \Delta E_i < -\ln R$, where β and R are the inverse temperature increased during annealing and a random number in the interval $(0, 1)$, respectively. In a step of SA, we sequentially update spin variables s_i ³⁹.

In numerical experiments, we measure computational costs of finding exact solutions as follows. We randomly generate 100 3R3X instances for each N . For these instances, we run the above mentioned SB and SA many times with different initial conditions or random numbers, and obtain probabilities of finding exact solutions, P . Then, using the number of steps in a run, N_s , we estimate the number of steps necessary to obtain exact solutions with a probability of 99% (step-to-solution) by^{11,20}

$$S = N_s \frac{\log 0.01}{\log(1 - P)}. \quad (12)$$

A smaller S indicates that an algorithm provides an exact solution more efficiently (or faster if computation time for each step is assumed to be the same).

We set the parameters as follows. For SB, $a_0 = 1$, and $a(t)$ is increased linearly. To normalize the term $c f_i$ in Eq. (2), we give c by⁴⁰

$$c = c_1 \left(\frac{1}{\nu} \sum_{i=1}^{\nu} f_i^2 \right)^{-1/2}, \quad (13)$$

where c_1 and ν are a constant parameter and the number of spin variables, respectively (ν are $2N$ and N for the second- and third-order SBs, respectively). We optimize N_s for each N , and $(\Delta t, c_1)$ for certain large values of N ,

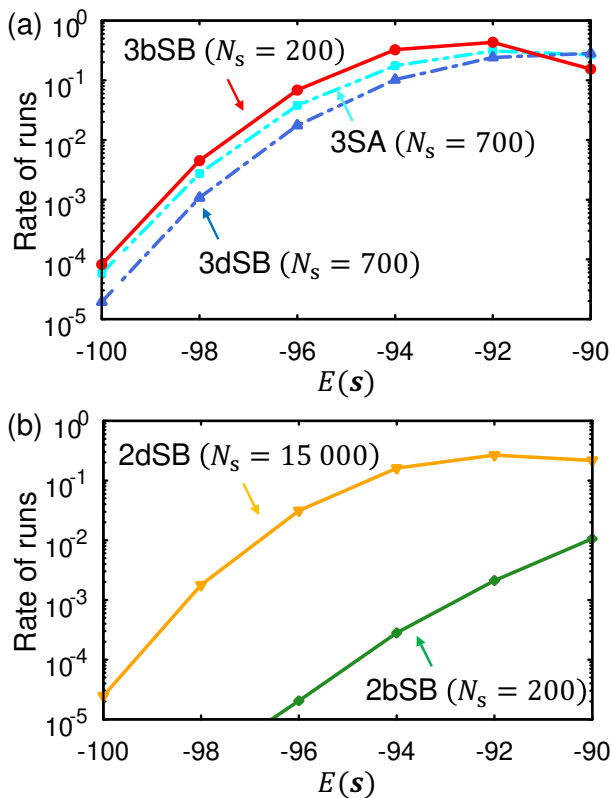


FIG. 1. Distributions of a third-order cost function $E(\mathbf{s})$ for a 3R3X instance with 100 spin variables. (a) 3bSB, 3dSB, and 3SA. (b) 2bSB and 2dSB. The lines are eye guides. The numbers of steps N_s are shown in the parentheses. Here, N_s and the following parameters are determined to minimize step-to-solution S . The parameters are $(\Delta t, c_1) = (1.1, 0.7)$ for 3bSB, $(0.7, 1.1)$ for 3dSB, $(0.8, 0.9)$ for 2bSB, $(0.7, 1.6)$ for 2dSB, and $\beta_1 = 2$ for 3SA.

to minimize the median of S for the 100 instances²². Initial x_i and y_i are generated by uniform random numbers in the interval $(-1, 1)$. To suppress a statistical error in P , the number of runs N_r is set to be large such that $N_r P \gg 1$ ¹⁹, though this condition is not necessarily met for the largest N in this work owing to limitations of computational resources. For SA, β is linearly increased from zero to a final value β_1 , and β_1 and N_s are optimized as in SB.

We first present typical distributions of $E(\mathbf{s})$ for a 3R3X instance, for which 3bSB gives S near the median of the 100 instances. Figure 1 shows the distributions by the rates of runs resulting in $E(\mathbf{s})$. A higher value of the rate means a higher probability of finding solutions with certain accuracy, though here the parameters are optimized to minimize S as mentioned above and the rates can be improved by increasing N_s . Interestingly, Fig. 1(a) shows that the rate for small $E(\mathbf{s})$ is higher for 3bSB than for 3dSB despite smaller N_s for 3bSB. On the other hand, Fig. 1(b) shows that the rate is higher for 2dSB than for 2bSB in accordance with much larger N_s for 2dSB. As shown in Fig. 1(a), the rate for 3SA is

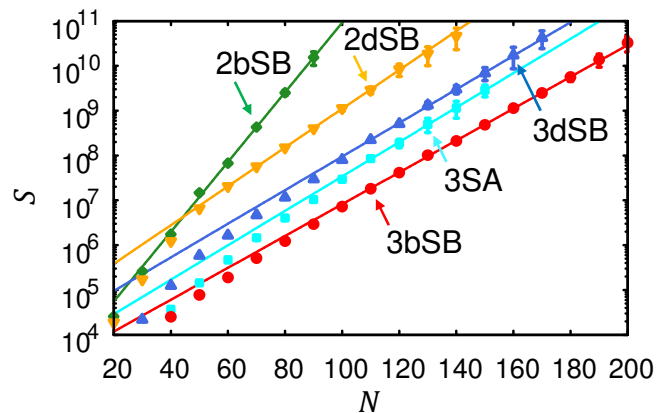


FIG. 2. The medians of step-to-solution S for 100 3R3X instances as functions of the number of spin variables N . The lines and error bars show fittings by Eq. (14) and statistical errors¹⁹, respectively. Parameters $\Delta t, c_1$, and β_1 are the same as in Fig. 1.

between those of 3bSB and 3dSB. These rates and N_s suggest the highest performance of 3bSB.

We next evaluate the results for 100 3R3X instances. Figure 2 shows the medians of S as functions of N . All the algorithms exhibit exponential increases of S with N . The values of S are smaller for third-order bSB and dSB than for the second-order ones. Among the second-order ones, 2dSB gives smaller S than 2bSB, which is consistent with a reported result that dSB more often reaches exact solutions for the Ising problem¹⁹. Among the third-order SB, in contrast, 3bSB shows smaller S than 3dSB. The higher performance of 3bSB might be because bSB can rapidly converge to a local minimum of a cost function¹⁹ and a local search algorithm is effective for the 3R3X problem^{22,35,36}. A comparison between 2bSB and 3bSB suggests that the local search by bSB is especially effective when directly applied to third-order cost functions with fewer spin variables. 3SA results in S between those of 3bSB and 3dSB, indicating that 3bSB is superior to 3SA.

Scaling can be measured by exponents α and β such that

$$S \simeq 10^{\alpha N + \beta}, \quad (14)$$

for large N ²². A smaller α allows an algorithm to be applied to larger instances. We fit the medians of S by Eq. (14) with the least squares method as the lines in Fig. 2. Here, only the data for intermediate N are used for the fittings, because errors due to finite-size effects and statistical errors are large for small and large N , respectively²². Table I shows α and β . The value of α for 3bSB is the smallest. α for 3dSB is a little larger than it, and α for 2dSB is significantly larger. α for 2bSB is by far the largest. The value of α for 3SA is larger than those for 3bSB and 3dSB. These α demonstrate that 3bSB scales the best among these algorithms.

Finally, we compare α with the results of Ref. 22, where various Ising machines are benchmarked using the

TABLE I. Scaling exponents. The numbers in the parentheses are standard deviations in the least squares method.

	3bSB	3dSB	3SA	2bSB	2dSB
α	0.0355(2)	0.0375(6)	0.0384(6)	0.078(1)	0.0433(2)
β	3.36(4)	4.23(8)	3.69(8)	3.19(9)	4.72(2)

3R3X problem expressed by second-order cost functions. Among the Ising machines, Digital Annealer reported the smallest exponent corresponding to $\alpha = 0.0370(8)$ ⁴¹. Compared with this value, α for 3bSB seems to be smaller. α for Simulated Bifurcation Machine (provided by Toshiba Digital Solutions Corporation⁴²) corresponds to 0.0434(12), which coincides with that for 2dSB in this work within the range of errors. This coincidence may support the validity of our evaluation. In Ref. 22, a quasi-greedy algorithm called SATonGPU^{22,35,36} is also compared, which is specialized for the 3R3X problem and deals with third-order cost functions directly. As a result, SATonGPU provided the exponent corresponding to $\alpha = 0.0341(2)$ ⁴³, which is close to an estimated optimal exponent³⁵. The value of α for SATonGPU is smaller than α for 3bSB in our work, but the difference is fairly small. This implies that 3bSB can achieve almost optimal scaling even though 3bSB is not specialized for the 3R3X problem.

In summary, we have demonstrated that third-order SB can perform better than second-order one for a 3R3X problem. Although 2dSB provides better performance than 2bSB, 3bSB instead does better than 3dSB. Furthermore, we have shown that 3bSB can be superior to 3SA. These results indicate that higher-order SB can be useful for solving combinatorial optimization problems expressed naturally by higher-order cost functions. Since we have formulated the higher-order SB by matrix-vector operations, we expect that the higher-order SB may be accelerated by parallel processing with, e.g., GPUs and FPGAs.

We thank Y. Sakai, T. Kashimata, K. Tatsumura, and R. Hidaka for helpful discussions.

¹F. Barahona, J. Phys. A: Math. Gen. **15**, 3241 (1982).

²A. Lucas, Front. Phys. **2**, 5 (2014).

³N. Mohseni, P. L. McMahon, and T. Byrnes, Nat. Rev. Phys. **4**, 363 (2022).

⁴T. Kadowaki and H. Nishimori, Phys. Rev. E **58**, 5355 (1998).

⁵M. W. Johnson et al., Nature **473**, 194 (2011).

⁶A. Marandi, Z. Wang, K. Takata, R. L. Byer, and Y. Yamamoto, Nat. Photonics **8**, 937 (2014).

⁷S. Kirkpatrick, C. D. Gelatt, and M. P. Vecchi, Science **220**, 671 (1983).

⁸M. Yamaoka, C. Yoshimura, M. Hayashi, T. Okuyama, H. Aoki, and H. Mizuno, IEEE J. Solid-State Circuits **51**, 303 (2016).

⁹M. Aramon, G. Rosenberg, E. Valiante, T. Miyazawa, H. Tamura, and H. G. Katzgraber, Front. Phys. **7**, 48 (2019).

¹⁰H. Goto, K. Tatsumura, and A. R. Dixon, Sci. Adv. **5**, eaav2372 (2019).

¹¹T. Leleu, F. Khoyratee, T. Levi, R. Hamerly, T. Kohno, and K. Aihara, Commun. Phys. **4**, 266 (2021).

¹²H. Goto, Sci. Rep. **6**, 21686 (2016).

¹³S. Puri, C. K. Andersen, A. L. Grimsmo, and A. Blais, Nat. Commun. **8**, 15785 (2017).

¹⁴H. Goto, J. Phys. Soc. Jpn. **88**, 061015 (2019).

¹⁵T. Kanao and H. Goto, npj Quantum Inf. **7**, 18 (2021).

¹⁶K. Tatsumura, A. R. Dixon, and H. Goto, IEEE Int. Conf. Field Programmable Logic and Applications (FPL), 2019, p. 59.

¹⁷Y. Zou and M. Lin, ACM/SIGDA Int. Symp. Field-Programmable Gate Arrays (FPGA '20), 2020, p. 65.

¹⁸K. Tatsumura, M. Yamasaki, and H. Goto, Nat. Electron. **4**, 208 (2021).

¹⁹H. Goto, K. Endo, M. Suzuki, Y. Sakai, T. Kanao, Y. Hamakawa, R. Hidaka, M. Yamasaki, and K. Tatsumura, Sci. Adv. **7**, eabe7953 (2021).

²⁰T. Kanao and H. Goto, Commun. Phys. **5**, 153 (2022).

²¹H. Oshiyama and M. Ohzeki, Sci. Rep. **12**, 2146 (2022).

²²M. Kowalsky, T. Albash, I. Hen, and D. A. Lidar, Quantum Sci. Technol. **7**, 025008 (2022).

²³K. Steinhauer, T. Fukadai, and S. Yoshida, arXiv:2009.08412 (2020).

²⁴J. Cohen and C. Alexander, arXiv:2011.01308 (2020).

²⁵K. Tatsumura, R. Hidaka, M. Yamasaki, Y. Sakai, and H. Goto, IEEE Int. Symp. Circuits and Systems (ISCAS), 2020, p. 1.

²⁶T. Zhang, Q. Tao, and J. Han, IEEE Int. SoC Design Conf. (ISOC), 2021, p. 288.

²⁷N. Matsumoto, Y. Hamakawa, K. Tatsumura, and K. Kudo, Sci. Rep. **12**, 2669 (2022).

²⁸W. Zhang and Y.-L. Zheng, arXiv:2210.14660 (2022).

²⁹V. Kolmogorov and R. Zabih, IEEE Trans. Pattern Analysis and Machine Intelligence **26**, 147 (2004).

³⁰H. Ishikawa, IEEE Trans. Pattern Analysis and Machine Intelligence **33**, 1234 (2011).

³¹R. Xia, T. Bian, and S. Kais, J. Phys. Chem. B **122**, 3384 (2018).

³²N. Dattani, arXiv:1901.04405 (2019).

³³J. Fujisaki, H. Oshima, S. Sato, and K. Fujii, Phys. Rev. Res. **4**, 043086 (2022).

³⁴I. Hen, Phys. Rev. Appl. **12**, 011003 (2019).

³⁵M. Bernaschi, M. Bisson, M. Fatica, E. Marinari, V. Martin-Mayor, G. Parisi, and F. Ricci-Tersenghi, Europhys. Lett. **133**, 60005 (2021).

³⁶M. Bellitti, F. Ricci-Tersenghi, and A. Scardicchio, Phys. Rev. Res. **3**, 043015 (2021).

³⁷B. Leimkuhler and S. Reich, *Simulating Hamiltonian Dynamics* (Cambridge University Press, Cambridge, 2004).

³⁸M. Leib, P. Zoller, and W. Lechner, Quantum Sci. Technol. **1**, 015008 (2016).

³⁹S. V. Isakov, I. N. Zintchenko, T. F. Rønnow, and M. Troyer, Comput. Phys. Commun. **192**, 265 (2015).

⁴⁰Y. Sakai, H. Goto, K. Tatsumura, K. Endo, and M. Suzuki, International patent application PCT/JP2020/006841 (20 February 2020).

⁴¹In Ref. 22, scaling is given with respect to $\nu = 2N$.

⁴²See <https://aws.amazon.com/marketplace/pp/prodview-f3hbaz4q3y32y> for Simulated Bifurcation Machine by Toshiba Digital Solutions Corporation; accessed 21 November 2022.

⁴³In Ref. 35, scaling is expressed with e^{aN} .